View metadata, citation and similar papers at core.ac.uk
brought to you by CORE
provided by Loughborough University Institutional Repository

Microstructure of Ti-6Al-4V produced by selective laser melting

M Simonelli[1], Y Y Tse[1] and C Tuck[2]

[1] Department of Materials, Loughborough University, Loughborough, LE11 3T, UK.

[2] School of Mechanical and Manufacturing Engineering, Wolfson Building, Loughborough University, Loughborough LE11 3TU, UK

E-mail: M.Simonelli@lboro.ac.uk

Abstract. Ti-6Al-4V is the most widely used titanium alloy. Manufacturing of Ti-6Al-4V components using novel additive processing techniques such as selective laser melting is of great interest. This study focuses on the microstructure characterization of Ti-6Al-4V components produced by selective laser melting (SLM) with full (Ti-6Al-4V base plate) and partial (Ti-6Al-4V needle-shaped structures) support. The starting material, a plasma atomised powder, and the component products are studied using various microscopy techniques including optical, scanning and transmission electron microscopy and electron backscattered diffraction. Powder particles are fully dense, possess a spherical shape and are composed of acicular α phase. The as-built material shows oriented acicular martensitic phase with well defined columnar grains. The morphology of martensitic phase and the microstructural evolution will be discussed in relation to the SLM processing parameters employed and the different cooling rates experienced by the components.

Introduction

Recently, selective laser melting (SLM) of powder materials has been proposed as an alternative manufacturing route to produce Ti-6Al-4V (Ti64) components, as this process, similar to other rapid prototyping techniques, allows a production of near-net-shape parts with high material utilization and freedom of design [1]. SLM products do not require further downstream processes and therefore this technology is suggested to reduce costs and lead time on production. One of the most attractive advantages offered by the SLM manufacturing technique is that it allows tailoring, to some extent, the microstructure of the component by tuning the process parameters in a strategic manner [2]. In particular, it has been demonstrated that the quantity of energy delivered to the metallic powders (i.e. energy density) plays a crucial role on the microstructure of the SLM products [1,2]. When it comes to Ti-6Al-4V, the fundamental question is whether the SLM Ti64 products could have mechanical properties comparable to the wrought or cast Ti64. The intrinsic characteristic of the SLM technology is the high solidification rate experienced by the powder material which determines, in turn, a characteristic fine microstructure with low ductility [3].This study is aimed at understanding the origin and the evolution of the microstructure of Ti-6Al-4V parts produced by SLM. Attention was focused on the stability of the process and the role of the supporting structures on the microstructural evolution of the built components.

Materials and methods

The powder material used for this study was Ti-6Al-4V grade 23 type 5 with nominal chemical composition as shown in Table 1. All the SLM components were built using a MTT SLM 250 machine; the adopted process parameters are listed in Table 2. The volumetric energy density E was calculated as:

$$E = \frac{P}{v\,d\,h}$$

where P is the laser power (W), v is the scanning velocity (μm/s) given by the ratio of the point distance (μm) to the exposure time (μs), h is the hatch spacing (μm) and d is the layer thickness (μm). The parts were built in a controlled Ar atmosphere to avoid any possible oxygen contamination. The build plate under the powder bed was kept at a temperature of 65°C in order to reduce the residual stresses that might develop during the process. Simple cubic specimens with volume of 1 cm^3 were built. SLM of Ti-6Al-4V powders was carried out directly on top of a Ti-6Al-4V build plate and onto Ti-6Al-4V needle-shaped supports, respectively, using the same scanning strategy. Different supports provided different contact area and hence different thermal histories to the built components. The microstructural evolution of the SLM cubes on different heat sink was studied using optical microscopy, scanning and transmission electron microscopy (SEM and TEM). Backscattered electron diffraction (EBSD) was used to study the phase and orientation distribution of Ti64 powder and built parts. The samples were ground on SiC papers and polished with a diamond paste of 9 μm first, and a SiO_2-H_2O_2 solution after. Kroll's reagent was used as etching agent. The 3-mm diameter TEM foil were prepared using a twin-jet electropolisher in an electrolyte of perchloric acid (10%), ethanol and distilled water at -20°C. TEM was carried out using a Jeol 2000FX microscope operated at 200kV.

Table 1 Chemical composition of Ti-6Al-4V powders

Element	N	C	H	Fe	O	Al	V	Ti
wt%	0,03	0,08	0,01	0,02	0,13	6,50	4,50	Bal.

Table 2 Process parameters

Laser Power [W]	200
Hatch spacing [mm]	180
Layer thickness [mm]	50
Point distance [mm]	50
Exposure time [ms]	251
Energy Density [J mm^{-3}]	11.1 * 10^{-5}

Results and discussion

The Ti64 powder particles were produced by a plasma atomization process and therefore appear spherical, smooth, fully dense and with few satellites as shown in Figure 1a. The measured particle size distribution was within 15 and 70 μm, however, about 75% of the examined particle size ranged between 25 to 50 μm. Preliminary EBSD results show that the particles are randomly orientated and contain lamellar α phase (Figures 1b and c). Due to the line and layer-wise building strategy, the microstructure of the SLM samples shows different morphology when viewing from different planes. A commonly used coordinate system is the scanning plane x-y and the built direction *z*. The microstructure of the top view (*x*-*y* plane) consists of features that are correlated to the scan strategy and in particular to the heat conducting direction. Coherently to what has been reported by Thijs et al. [1], individual laser scan tracks can be identified on Figure 2 which shows the top surface of the specimen built on needle supports. Each laser scan interacts with a portion of material about 235±15 μm wide. When the top surface is polished and etched it reveals a fully dense microstructure (no pores are observed) with relatively coarse alpha phase where needles of martensitic alpha emerge as dark contrast. It should be noted that the top surface was scanned twice in order to improve the overall geometrical accuracy and surface finish of the component. This morphology is similar to what Ahmed et al. have reported [4].

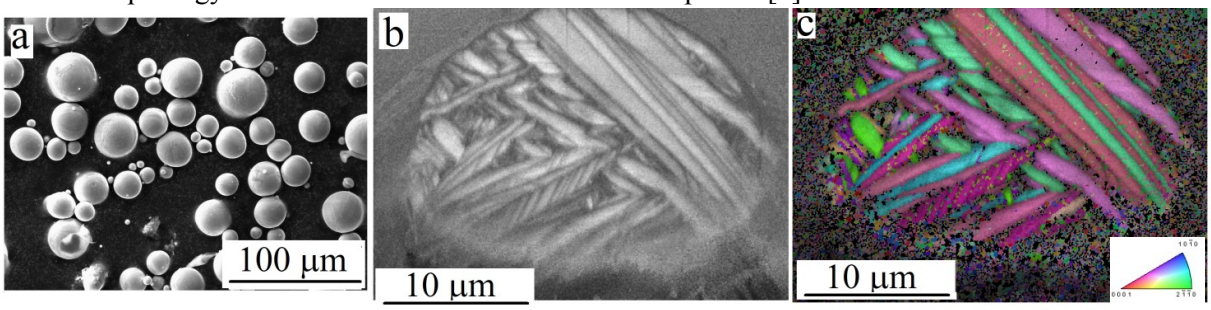

Figure 1. a) SEM micrograph of Ti-6Al-4V powder particles, b) EBSD image quality map of a randomly selected particle , c) Orientation map of the particle and the inset shows the inverse pole figure colour scheme.

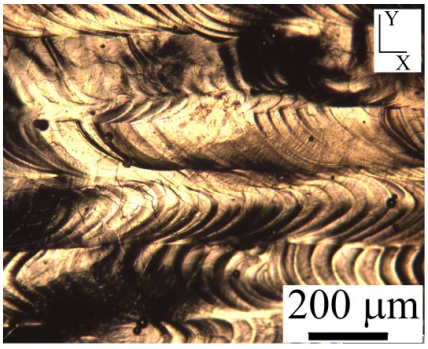

Figure 2. Top surface of the as-built component

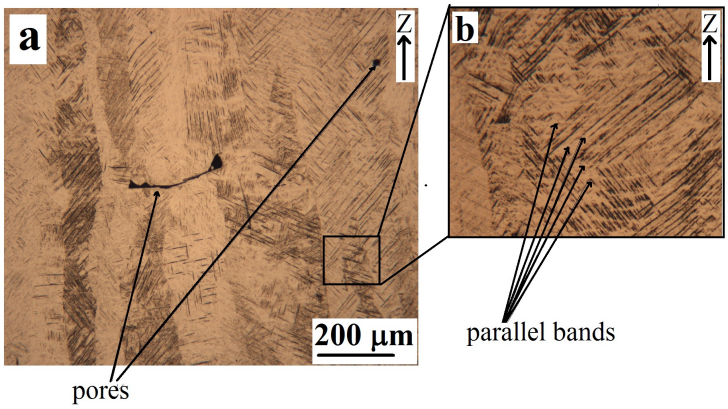

Figure 3. a) Frontal cross-section exhibiting columanar grains and pores, b) parallel bands as marked by arrows

Beta phase was not detected by X-ray diffraction and EDS analysis as a result of the high cooling rate that occurs during SLM. The microstructure of the bottom surface (x-y plane) is slightly different from that observed on the top surface: spherical pores can be noted and the volumetric fraction of acicular martensite increases. The microstructure of the front and side cross-sections (*y-z* and *x-z* plane, respectively) reveals information regarding to the thermal history that the layers have experienced. The observed porosity has two characteristic morphologies: pores are flat and oriented in the x-y plane or spherical (pin-hole morphology) as shown in Figure 3a. As re-heating of the previously solidified layers gives rise to re-growth, morphology and microstructure of the component differ along the build height. Columnar grains are observed in cross sections (Figure 3a). According to the present results, two different regions can be identified: 1) a region that goes from the middle to the top portion of the specimen and includes the external surfaces (wall surfaces) 2) a region representative for the first layers in contact with the supportive needles (bottom region). Near the external surfaces (wall surfaces) and from the middle to the top region, the morphology exhibits a colony pattern with parallel acicular needles (Figure 4a). These etch resistant needles are considered martensitic regions between alpha lamellae [5]. At higher magnification it is possible to distinguish smaller needles that can be considered as secondary α structures, probably grown because of the subsequent heating and cooling that occur during the SLM process. Most of the acicular needles are arranged at ± 45° to the z-axis in accord with the preferential planes of crystallographic growth (Figures 3a and 4a). Further TEM investigations and XRD are required to confirm the crystal structure and orientation of the martensitic needles. Beside the slight crystallographic difference, it has been reported that α' structures are generally contain a high dislocation density, sometimes twins and higher content in V with respect to HCP α lamellae as shown in Figures 5 a and b [5]. In the bottom region, the morphology of the martensitic α needles shows a basket-weave pattern (Figure 4b); as it can be noticed, some of the acicular needles appear entangled as a result of competitive growth. This morphology is coherent to that described by Baufeld et. al in wire deposited Ti-6Al-4V specimens [6].

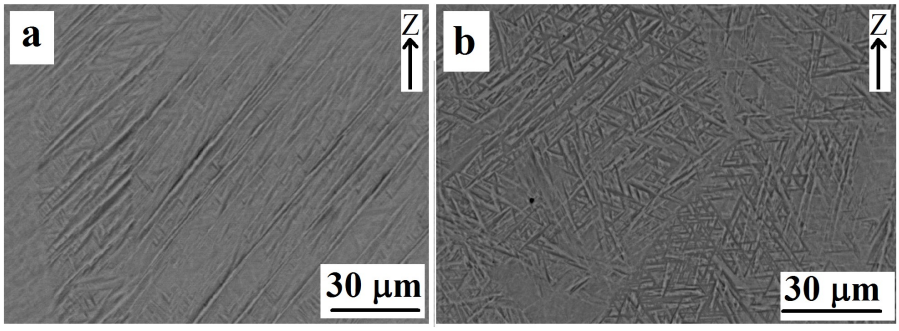

Figure 4. a) Typical wall surface and top region microstructural morphology, b) basket-weave morphology found prevalently in the bottom portion of the specimens

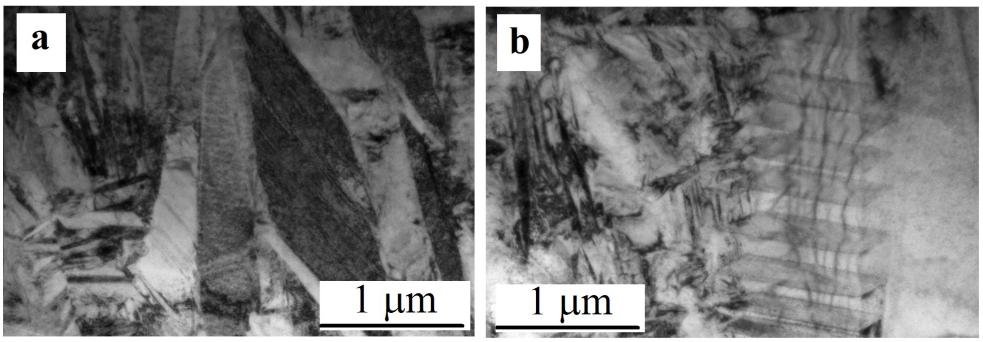

Figure 5. Bright field TEM micrograph showing a) α lamellae, b) stacking faults within the lamellae

In general, oriented structures were observed at wall surfaces while basket-weave morphology was present from the bottom to the middle region of the specimens. It is noteworthy that basket-weave morphology is not observed in correspondence of the needle supports but just in the zone that where in contact with the loose powder. Since the heat conduction is lower in the zones without needle supports, the basket-weave structure might be associated with a slower cooling rate and different thermal cycling. In the middle portion, the processed components show a layered structure and elongated columnar grains which grow across the layer (Figure 3a). The columnar grains are a result of epitaxial growth of the previous layer upon successive laser scans [7].Contrary to the result obtained by Thijs et al. [1], the observed columnar grains do not possess an inclination with respect to *z* direction (Figure 3a): this is probably due to the different adopted scanning strategy. The average width of the columnar grain is of 210±50 μm. Interestingly, the ratio of the scan track width to the columnar grain width is approximately unitary. Finally, the middle portion of specimens displays periodic bands parallel to the base substrate (Figure 3b): these parallel bands, tend to disappear near the top surface of the components. Focused ion beam assisted TEM and EDS analysis are on-going to understand whether these structure could be inter-metallic compounds (i.e. where micro-segregation has occurred) or areas with a different specific crystallographic orientation. The microstructures of the samples built on the Ti64 plate show similar feature as the ones built on needle supports; however, smaller pores are observed.

Conclusion

Selective laser melting has proved to be a new and promising method to directly fabricate metal parts. In this work, Ti-6Al-4V cubic blocks were built and characterized; the resulting microstructure is different from that observed in cast or wrought materials but given its complexity further investigations are required. The microstructural features in the as built SLM component include fine martensitic and secondary alpha phase, oriented columnar grains (that probably imply a degree of anisotropy in the build direction), flat defects (pores) and periodic band structures.

References

[1] Thijs L, Verhaeghe F, Craeghs T, Humbeeck JV, Kruth JP. 2010 *Acta Materialia* **58** 3303-3312.
[2] Yadroitsev I, Thivillon L, Bertrand P, Smurov I.. 2007 *Applied Surface Science* **254** 980-983.
[3] Facchini L, Magalini E, Robotti P, Molinari A, Hoeges S, Wissenbach K. 2010 *Acta Materialia* **58** 3303-3312.
[4] Ahmed T, Rack H. *Materials Science and Engineering A* 1998 **243** 206-211.
[5] Qazi J, Rahim J, Fores F, Senkov O, Genc A. 2001 *Metallurgical and Materials Transactions A* **32** 2453-2463.
[6] Baufeld B, Brandl E, van der Biest O. J Mater Process Technol 2011 **211** 1146-1158.
[7] Kelly S, Kampe S. 2004 *Metallurgical and Materials Transactions A* **35** 1861-1867